



EUROPEAN ORGANIZATION FOR NUCLEAR RESEARCH

CERN/EP 80-36  
25.3.1980

A LARGE ACCEPTANCE SPECTROMETER  
TO STUDY HIGH-MASS MUON PAIRS

CEN-Saclay<sup>1</sup>-CERN, Geneva<sup>2</sup>-Collège de France, Paris<sup>3</sup>-  
Ecole Polytechnique, Palaiseau<sup>4</sup>-Laboratoire de l'Accélérateur Linéaire, Orsay<sup>5</sup>

J. Badier<sup>4</sup>, J. Boucrot<sup>5</sup>, G. Burgun<sup>1</sup>, R. Busnello<sup>5</sup>, O. Callot<sup>5</sup>, Ph. Charpentier<sup>1</sup>,  
M. Crozon<sup>3</sup>, D. Décamp<sup>2</sup>, Ph. Delcros<sup>4</sup>, P. Delpierre<sup>3</sup>, A. Diop<sup>3</sup>, R. Dubé<sup>5</sup>,  
B. Gandois<sup>1</sup>, R. Hagelberg<sup>2</sup>, M. Hansroul<sup>2</sup>, R. Hammarström<sup>2</sup>, W. Kienzle<sup>2</sup>,  
A. Lafontaine<sup>1</sup>, P. Le Dû<sup>1</sup>, J. Lefrançois<sup>5</sup>, Th. Leray<sup>3</sup>, R. Lorenzi<sup>2</sup>, Y. Malbequi<sup>1</sup>,  
G. Matthiae<sup>2</sup>, A. Michelini<sup>2</sup>, Ph. Miné<sup>4</sup>, H. Nguyen Ngoc<sup>5</sup>, S. Palanque<sup>1</sup>,  
O. Runolfsson<sup>2</sup>, P. Siegrist<sup>1</sup>, J. Timmermans<sup>2\*</sup>, J. Valentin<sup>3</sup>, R. Vanderhaghen<sup>4</sup>,  
S. Weisz<sup>2</sup>.

ABSTRACT

This paper gives the outlines of the NA3 large acceptance magnetic spectrometer equipped with multiwire proportional chambers running at the CERN-SPS in an extensive study of the production of high mass muon pairs by hadronic beams. A special feature of this experiment is the powerful and efficient trigger and data acquisition system which allows operation of the spectrometer with intense beams, yielding at the same time low trigger rate and high proportion of good events. Some aspects of the off line analysis program are also described.

(Submitted to Nuclear Instruments and Methods)

---

\*) Now at NIKHEF-H, Amsterdam, The Netherlands.

## 1. INTRODUCTION

In this paper we describe the apparatus used to perform a beam dump experiment on production of massive muon pairs by high energy (150-400 GeV) hadron beams at the CERN Super Proton Synchrotron. The experiment known as NA3, has by now run successfully for one and a half years collecting  $\sim 2 \cdot 10^7$  triggers and yielding a substantial amount of new physics data<sup>(1,2,3)</sup>. The general layout of the spectrometer is shown in fig.1. The main technical elements of the experiment and their features are described in this paper in some detail, namely: a) the high intensity hadron beam (sect.2); b) the targets and the beam dump (sect.3); c) the magnetic spectrometer equipped with multiwire proportional chambers and counter hodoscopes (sect.4,5,6); d) the high rejection trigger system conceived to select events of high dimuon mass by means of two cathode read-out proportional planes of fine cell structure (sect.7); e) a powerful on-line data acquisition system (sect.8); f) a fast and efficient off-line analysis program for event reconstruction (sect.9).

## 2. THE HADRON BEAM

The NA3 experiment is using the H8 beam line in its high transmission mode ( $\Delta p/p = \pm 1.4\%$ ) to provide the experiment with maximum flux of beam particles. The H8 beam is derived from the T4 target operated with the SPS 400 GeV extracted proton beam and it reaches the NA3 experiment located in the EHN1 experimental hall after a path of approximately 500 meters. The beam line is fully instrumented with beam control equipment as well as beam detectors. Our experiment has made constant use of particle identification with Cerenkov counters (two differential counters called CEDAR's<sup>(4)</sup> and two gas threshold counters) and beam profile monitors. The beam elements as well as the beam controls and detectors are provided and operated by the CERN-SPS EA group. A description of the beam line and beam detectors can be found in ref. 5.

Table 1 summarizes the various beam energies used in our experiment together with corresponding particle fluxes, T4 target lengths and the beam composition as measured by the Cerenkov counters. The beam spot size was smaller than 12 mm diameter at all energies. The intensities indicated in Table 1 are usually the maximum values which could be tolerated either

by the beam Cerenkov counters and/or by the experiment trigger. The effective spill time for the 400 GeV proton extraction was 800 msec on the average. Notice that the intensities at +200 GeV are obtained by inserting a 2 meter CH<sub>2</sub> absorber in the beam in order to increase the  $\pi^+$  to proton ratio. Furthermore in the case of -150 GeV operation the relatively short T4 target length of 30 cm corresponds to an optimized ratio  $\bar{p}$  to  $\pi^-$ . The centering of the beam on our experimental target has been stable to  $\pm 0.5$  mm. An important requirement for the measurement of the absolute cross section is a precise monitoring of the beam intensity. This is achieved by two gas (argon) ionization chambers<sup>(6)</sup> placed on the beam approximately 10 m upstream of the experiment. These chambers give linear response in the intensity range  $10^6$ - $10^9$  particles/sec and are calibrated by counting the beam flux with a scintillation counter telescope up to a few times  $10^6$  particle/sec. This allows to monitor the beam intensity during data taking to an accuracy of a few percent. In addition a beam intensity monitor made of a telescope of three scintillation counters looking at the target at an angle of  $\sim 60^\circ$  was also used. A beam halo veto counter H (see fig.2) is mounted approximately 10 m upstream of the targets to reject triggers induced by muons of the beam halo.

### 3. TARGETS AND BEAM DUMP

#### 3.1 Targets

Two targets were mounted at the experiment. A 6 cm long, 12 mm diameter platinum target, was positioned 40cm in front of the beam dump. The second target, 30 cm of liquid hydrogen, was positioned 45 cm upstream of the platinum target. This arrangement allowed us to collect simultaneously a large number of massive muon pairs produced on platinum nuclei and a lower statistics sample of similar events produced on free protons. The assignment of events to the appropriate targets is performed off line (see sect.9.3). To minimize the fraction of events with an ambiguous target assignment a Cerenkov counter is used to flag the interactions produced in the hydrogen target. This counter I1 is mounted between the two targets (see fig.2) 35 cm downstream of the hydrogen target. It is made of perspex with a 2 cm Pb front plate to convert  $\gamma$  rays produced at the hydrogen target and a 3 mm Cu back plate to shield against back scattering from the platinum target. To minimize the variations of the photomultiplier

gain the HV is kept low and the counter signal is amplified 20 times. The counting rate as a function of the high voltage shows a distinct plateau at about 80% efficiency corresponding to the interactions in hydrogen, followed by a rapid rise due to backscattering from the platinum target. The I1 counter is operated on the plateau and at a counting rate of typically 7% of the beam flux. The efficiency of I1 for interactions in the platinum target is 15%.

### 3.2 Beam dump

The beam dump configuration was determined taking into account conflicting requirements from the experiment : a short length to preserve large acceptance of the spectrometer; large absorption power to strongly reduce the particle flux through the apparatus; small multiple scattering for a good dimuon mass resolution and finally a suitable material for operation inside the magnet.

The dump used in the experiment is made of a 1.5 m long block of stainless steel (see fig.3). It contains a central conical core of tungsten and uranium conceived to absorb more effectively the hard component of the hadronic shower along the beam axis. Two apertures of the cone can be used : 20 and 30 milliradians. The stainless steel surrounding the central core is chosen for its relatively good absorption power together with a reasonable low multiple scattering for penetrating muons. Additional muon filtering is provided for by a 1.8 m thick iron absorber placed in front of the last counter hodoscope T3, at the end of the spectrometer.

The design of the dump proved to be quite adequate for the needs of the experiment : the charged particle flux behind the dump was measured to be ~20% of the incident beam intensity; its space distribution at the exit of the dump shows a broad maximum with a FWHM of about 35 cm. The centering of the beam on the dump axis is not critical for a lateral displacement of less than 1 cm.

All these experimental features were found to be in satisfactory agreement with the predictions of a Monte Carlo simulation used for the design of the dump<sup>(7)</sup>. The dimuon events selected by the trigger system showed a multiplicity distribution sharply peaked around two particles. Nevertheless a rather flat tail extended towards very high multiplicities.

A large fraction of these events were shown to be electromagnetic showers most probably originating from bremsstrahlung emission by high energy muons traversing the iron of the dump or the yoke of the magnet. These events were subsequently suppressed in the trigger (see sect. 7.4).

#### 4. THE SPECTROMETER MAGNET

The spectrometer magnet is a superconducting dipole<sup>(8)</sup> with a cylindrical volume of useful magnetic field 2.5 m long and 1.6 m diameter. The main field component is vertical with a maximum value at the center of 1.67 Tesla at 90% of the maximum attainable current. The bending power in the central region is 4.1 Tesla-meter corresponding to a transverse momentum kick of 1.2 GeV/c for particles traversing the magnet.

#### 5. THE COUNTER HODOSCOPES

Three planes of counter hodoscopes T1, T2, T3 are used in the experiment (see fig.1 and 2).

The hodoscope T1 is mounted on the downstream face of the beam dump and it is divided into 12 elements, six above and six below the median horizontal plane. These elements have different sizes in order to be exposed approximately to the same particle flux. The dimensions of each half hodoscope correspond to an angular acceptance from 24 to 175 mrad in the vertical plane so that the central region -24 to +24 mrad remains uncovered; for the -150 GeV run, the addition of four counter elements improved the lower bound of the acceptance from 24 to 10 mrad. The signals derived from T1 are registered by TDC's in order to provide a precise timing reference for the events.

The hodoscope T2 is part of a calorimeter which was built to detect electrons in a subsequent stage of the experiment. It is placed in front of the iron absorber and behind the last multiwire proportional chamber unit. It is used in the present experiment as an ordinary hodoscope made of 42 horizontal strips. Each strip is made of two symmetric halves (left and right), each half being viewed by a photomultiplier. The angular acceptance in the vertical plane of T2 is  $\pm(4$  to 172) mrad.

T3, the largest of the three hodoscopes ( $6 \times 5.5 \text{ m}^2$ ), is mounted behind the iron absorber at the back of the spectrometer. It is made of 22 horizontal strips each being composed of two halves symmetric with respect to the median vertical plane. Its angular acceptance in the vertical plane is  $\pm(7 \text{ to } 165) \text{ mrad}$ s. T2 and T3 together have the purpose to select muons originated at the targets (see sect.7.2a).

## 6. THE MULTIWIRE PROPORTIONAL CHAMBERS

The NA3 spectrometer makes use of 31 proportional wire planes grouped in 6 units and corresponding to a total of 25,300 sense wires. The geometrical characteristics of the proportional chamber units are given in table 2. Chambers PC1<sup>(9)</sup> and PC2 are mounted immediately behind the beam dump inside the spectrometer magnet, hence they operate at a relatively high rate. For that reason they have fast amplifiers<sup>(10)</sup> mounted directly on the chamber frames or nearby ; the corresponding memory elements<sup>(11)</sup> are connected through long delay cables which provide a precise delay without dead time and allow the output signal of the amplifier to be gated by the fast pretrigger signal generated by an interaction occurred at the target (sect. 7.2). This signal arrives 260 nsec after the interaction at a rate of about  $10^5$  per second. The memory elements of all chambers are then strobed by the final trigger arriving  $\sim 600$  nsec after the interaction. Chamber units PC3 to PC6<sup>(12,13)</sup> which are operated at a relatively lower rate have both amplifiers and memory elements<sup>(14)</sup> mounted directly on the chamber frames. The chambers are read out via a set of 38 JCF20 Camac modules<sup>(15)</sup> (one per plane for PC1-PC4, two per plane for PC5 and PC6). All chambers are operated with a gas mixture consisting of 80% argon, 20% isobutane, 0,1% freon. The argon is bubbling through isopropyl alcohol at  $7^\circ\text{C}$ .

The cathodes of all chambers are made of mylar foils coated with thin layers of graphite. This choice has two essential advantages. First the wires are protected against damages, in the case of sparks, by the high resistance of the graphite. Second, the graphite properties allow the chamber to be exposed for a long time to intense radiation without deterioration of the cathode. (By now the proportional chambers have been operated for approximately 7000 SPS hours corresponding to an integrated particle flux of few times  $10^{13}$  over the chamber surface).

## 7. TRIGGER SYSTEM

### 7.1 Generalities

The main topic of this experiment being the study of high mass dimuons, our trigger system must select massive muon pairs ( $M_{\mu^+\mu^-} > 4 \text{ GeV}$ ) and at the same time reject low mass resonances (typically  $\rho^0$ ,  $\omega$ ,  $\phi$ ) which are produced with much larger cross sections. This can be done effectively by applying a cut to the transverse momentum  $p_T$  of one or both muons of the pair, since the dimuon mass  $M$  for a symmetric pair can be expressed as  $M = p_{T1} + p_{T2}$ . In practice this is accomplished by a system of two cathode read-out proportional chamber planes M1, M2 (see fig.2) and an associated hardware fast logic which computes within 110 nsec the vertical component of the transverse momentum of a particle having reached both planes.

Given the high overall interaction rate occurring at the target and the dump ( $10^7$  to  $10^9$  part/sec) this computation is performed only when an interaction yields at least two muons. This logical condition is provided by a fast coincidence between the elements of the three counter hodoscopes T1, T2, T3 and it is called pretrigger. In the two following sections we give details on the pretrigger and final trigger system.

### 7.2 Pretrigger

As mentioned in the preceding section the pretrigger corresponds to an interaction producing at least two muons detected in T3 behind the 1.8 m iron absorber. It is performed using the three counter hodoscopes T1, T2, T3 (see sect.5) with the following requirements :

a) a two-fold coincidence system between corresponding elements of hodoscopes T2 and T3 which defines the trajectories of two muons pointing approximately towards the targets. In particular we require each strip of T3 to be associated to four strips of T2 to allow for the multiple scattering through the 1.8 m iron absorber. A coincidence between these elements provides the signature of one muon in the trigger system and it is referred to in the remainder of this paper as  $\langle T2 \cdot T3 \text{ muon road} \rangle$ ; in the pretrigger we require at least two muons giving the signature of two  $\langle T2 \cdot T3 \text{ muon roads} \rangle$ ;

b) detection of at least one of the two muons by the hodoscope T1, mounted at the downstream face of the beam dump;

c) absence of any halo particle by a veto counter H mounted approximately 10 meters upstream of the experiment targets.

This pretrigger is generated 260 nsec after the interaction has occurred and it is used for the following purposes :

i) to gate the amplifiers of the proportional chambers PC1, PC2 and of the cathode read out chambers M1, M2 (sect.7.3) in order to reduce the otherwise excessive rate at the input of the memory elements;

ii) to latch the matrix logic conditions that are involved in the final trigger decisions, thus considerably reducing the trigger electronic losses.

### 7.3 Matrix logic description

The  $p_T$  selection is based on magnetic deflection in the horizontal plane of the muons produced at the target, followed by detection by the two cathode read-out proportional planes M1, M2 (see fig.2) and the subsequent  $p_T$  computation and selection by special fast electronic matrix logic<sup>(16)</sup>.

For this purpose the cathodes of the two proportional planes are each divided in 20 horizontal strips , 10 above and 10 below the median horizontal plane; that corresponds to an acceptance in the vertical component of the polar angle of  $\pm(15$  to  $165)$  mrad. The length of each strip is determined by the required acceptance of  $-60^\circ$  to  $+60^\circ$  in the azimuthal  $\phi$  angle measured from the vertical axis. Each strip is subdivided in 64 cells corresponding to equal intervals of  $\text{tg } \phi$ . The two proportional planes M1, M2 are mounted behind the spectrometer magnet at such positions that two corresponding cells are lined up in a straight line with the center of the platinum target.

The vertical component of the transverse momentum  $p_T^v$  of a particle produced at the target , traversing the two planes M1 and M2 and detected by the cells  $n_1$  and  $n_2$  respectively is given by :

$$p_T^v = \frac{A}{|n_1 - n_2|}$$

The signals from the cells, strobed by the pretrigger, are used to input 20 identical matrix logic units, one for each pair of corresponding strips. Each matrix, coding the right-most and left-most cells in M1 and M2, computes the corresponding values of  $\Delta n = |n_1 - n_2|$  and compares this value to a programmable lookup table giving four different fast NIM signals. In a given band the cells encoded by the matrix are the right-most and left-most ones, in this way the presence of one background track in the same band does'nt prevent the coding of the good track. In the case of the present setup  $\Delta n \leq 7$  corresponds to a  $p_T^V \geq 0.7$  GeV/c while  $\Delta n \leq 5$  corresponds to a  $p_T^V \geq 1$  GeV/c. To further improve the trigger rejection the fast outputs of one of the horizontal wire planes of PC2 are used in coincidence with the  $\langle T_2 \cdot T_3 \text{ muon roads} \rangle$  (see sect.7.2a)) to narrow down the path allowed to the muon generated at the target.

#### 7.4 The final trigger

In the final trigger each of the 20 matrix logic units is strobed by a corresponding pair of adjacent  $\langle T_2 \cdot T_3 \text{ muon roads} \rangle$  grouped in OR in order to take into account multiple scattering by the 1.8 m iron absorber. Two different triggers are then generated (see fig.4) :

a) Trigger 1 requires one muon of  $p_T^V > 1$  GeV/c within the M1, M2 acceptance and a second muon anywhere within the acceptance of the apparatus; it further imposes that the two muons are detected in two nonadjacent  $\langle T_2 \cdot T_3 \text{ muon roads} \rangle$  put in coincidence with one of the PC2 wire planes, thus rejecting single muons which give signals in two adjacent  $\langle T_2 \cdot T_3 \text{ muon roads} \rangle$ . This trigger represents ~90% of the total trigger rate.

b) Trigger 2 requires at least two muons of  $p_T^V \geq 0.7$  GeV/c corresponding to a transverse mass greater than  $1.4 \text{ GeV}/c^2$ . Furthermore, we demand for at least one of the muons to be detected by a  $\langle T_2 \cdot T_3 \text{ muon road} \rangle$  - in coincidence with PC2. This trigger represents ~40% of the total trigger rate and it overlaps partly with trigger 1.

An OR of Trigger 1 and Trigger 2 makes up the so-called final trigger, its main purpose being to select efficiently massive dimuon events ( $M_{\mu\mu} > 4 \text{ GeV}$ ) with unbiased  $p_T$  distribution.

These trigger requirements are efficiently fulfilled by unwanted showers produced at the end of the beam dump or in the magnet yoke, which have traversed a large number of M1, M2 cells. These events can be vetoed in the

trigger by means of the first section of the electron calorimeter which is mounted in front of T2 (see sect.5). This first section has horizontal strips, five meters long, viewed at both ends by a photomultiplier, thus allowing the output signals to be correctly timed by meantimers. Showers which trigger at least five adjacent strips are rejected in the trigger. A small fraction (1/10) of these events are retained in order to monitor off-line the loss of good events (about 1%). The on-line suppression of shower reduces the overall trigger rate by a factor of three. Typical rates, obtained during the actual data taking are listed in table 3 for operation at 200 GeV and an effective spill time of 800 msec. The final trigger occurs ~600 ns after the target interaction.

## 8. THE DATA ACQUISITION SYSTEM

The on-line system was designed to handle a maximum of 400 events per SPS cycle, each of 500 words of 16 bits. This means storing approximately 200 K words per SPS cycle in a buffer memory. In order to get rid of any space storage limitation of our data acquisition computer<sup>(17)</sup>, we have chosen the original solution of storing the data in an EXTERNAL CAMAC buffer with the subsequent transfer via the computer to the magnetic tape during the 9 second interval between SPS pulses. The information of each event, i.e. bit pattern of hodoscopes and triggers, wire hits in the chamber planes, ADC and TDC data, are encoded and stored by standard Camac units.

Anticipating a high data rate, we have optimized our read-out system in order to minimize the computer acquisition dead time. This has been achieved by handling data of the same type in autonomous Camac time sharing systems working in parallel. A schematic diagram of this system is given in fig.5. Instead of addressing with the same function a set of N identical Camac modules individually it is faster to address only one specific unit called CONCENTRATOR. Each concentrator controls several Camac crates filled with the same type of units. It executes simple Camac commands via a pseudo-Camac branch and the special controllers. We actually use three of these systems, two for the JCF20<sup>(18)</sup> readout modules, one for the ADC's and TDC's<sup>(19)</sup>. For each trigger the computer initializes the parallel readout of all modules in the pseudo-Camac branch. For ADC's and TDC's the concentrator suppresses all non pertinent data, e.g.

ADC's pedestals, thus reducing the data flow to about fifty 16 bit words for the overall 500 ADC and TDC channels.

A modified Crate Controller<sup>(20)</sup> is used to perform the read-out of each concentrator and to transfer the data to the external memory, at the maximum speed allowed by the Camac. Each external Camac buffer consists of 4 x 16 K words MOS memory units giving a total of 192 K words.

During the beam extraction time the buffer memories are filled with data under control of the PDP 11/45. During the rest of the SPS cycle, the computer recombines for each event the information coming from the external memories, performs consistency checks of the data, writes events on tape and fills a certain number of histograms. This on-line histogramming represents an efficient monitoring of the overall system of detectors and associated electronics (chamber efficiencies, patterns of counters etc.). On the average the length of an event written on tape is about 350 words. One tape (1600 bpi, 9 tracks) contains about 30,000 events.

Typical values for the performances of the data acquisition system are as follows :

- the time needed for the acquisition of one event is between 0.6 and 1 msec depending on the amount of data words;
- the maximum number of events per burst is ~400, for a 192 K words external memory;
- average number of events per burst in the present experiment : ~50;
- dead-time due to data acquisition : ~5%.

## 9. DATA PROCESSING

### 9.1 Pattern recognition

Pattern recognition is first performed for all tracks; muons are then identified by their impact in the T3 hodoscope, taking into account multiple scattering in the 1.8 m thick iron absorber.

The track finding procedure starts with the recognition of straight lines behind the magnet using the data from the chambers PC3 to PC6. The line finding is done successively in Y and X projections using an algorithm<sup>(21)</sup> specially developed for this experiment. The projections are found from

combinations of wires in planes of PC3 and PC6; all wires found in a successful combination are removed from the list of wires used for the line finding.

Y and X combinations are then matched in space using information from the inclined U and V planes, after which a straight line fit is performed to check the quality of the line.

The next step in the pattern recognition consists of tracking all straight lines through the magnetic field up to PC2 and PC1 where a point finding is performed with a loose constraint to the region of the targets, including the beam dump. Due to the tolerances which had to be kept in order to find points, multiple solutions are found for about 20% of the events.

The overall efficiency of the pattern recognition has been measured from visual scanning of reconstructed events, and is estimated to be  $98 \pm 1\%$ .

## 9.2 Estimation of track parameters

The total number of tracks for which track parameters had to be reconstructed was expected to be very large in this experiment. Hence, the following solution was found to be more economical in terms of computer time needed than conventional methods used in the estimation of the geometrical parameters of the tracks found.

Using the map of the fully measured magnetic field, many thousands of tracks were generated by our experiment simulation program (based on the CERN GEANT package)<sup>(22)</sup>. These tracks were then analysed by the principal component method<sup>(23)</sup> in order to obtain a set of functions giving for each track a parametrization of its momentum and its angles at the entrance of the magnetic field volume.

The number of generated tracks used in this analysis was such that the error in the estimation of the track parameters due to the method itself were by far inferior to the measurement error. The latter was, for the estimate of the momentum, found to be

$$\Delta p/p = 6.3 \cdot 10^{-4} \cdot p$$

### 9.3 Vertex finding

For events where two muons have been identified in the T3 hodoscope, a vertex finding is performed, which takes into account multiple scattering in the 1.5 m beam dump.

A first estimate of the vertex is obtained from the fitted tracks taking into account the errors due to multiple scattering and the beam constraints. This first determination shows a relatively clean separation of events produced in the platinum target from events produced in the dump for masses above  $2.5 \text{ GeV}/c^2$ . At masses of  $5 \text{ GeV}/c^2$  the separation becomes excellent (see fig.6). However the corresponding separation for events produced in hydrogen is worsened by the lower ( $\sim 1/50$ ) production probability and by the less favorable geometry of the hydrogen target relative to the platinum target (30 cm long as compared to 6 cm for the platinum target). To improve the separation of hydrogen events we use the time information of the I1 counter (see sect.3.1), recorded on a TDC. 80% of the hydrogen events together with 15% of the platinum events give a signal in the I1 counter, within  $\pm 3 \text{ ns}$  of the time reference. Without this information, about 2% of the  $J/\psi$  events produced in hydrogen are assigned to the platinum target, leading to a 2% contamination of the platinum events in the mass interval between 4-5 GeV. This contamination is reduced to about 0.5% by the use of the I1 counter.

A second estimate of the vertex is then obtained by computing for each target the probability of the event to originate from it, using the error on the first determination of the vertex. The probability is weighted by the I1 counter information and by the attenuation of the beam in the target. In addition a special weight is given to events for which, when assigned to the platinum target, the muon pair mass is compatible with the  $J/\psi$  mass. This is done in order to avoid a contamination of  $J/\psi$  events wrongly assigned to the dump and thus giving a substantially higher mass. Finally the most probable target is chosen and the vertex is assigned at the most probable point within this target.

Using this second estimate the invariant mass of the dimuon is computed, taking into account multiple scattering and  $dE/dx$  losses in the dump (the method is very similar to that used by Branson et al.)<sup>(24)</sup>. At  $200 \text{ GeV}/c$  the mass resolution (r.m.s) is 3.7% in the  $J/\psi$  region and about 4.5% in the  $T(9.4 \text{ GeV})$  region.

As an example of the quality of the results obtained in the present experiment we show in fig.9 the dimuon mass spectrum measured with 200 GeV  $\pi^+$ . A large  $\psi$  signal is observed accompanied by a clear T peak. This is the first evidence of T produced by  $\pi$  mesons<sup>(1)</sup>.

#### 9.4 Identification of beam particles

Beam particles are identified by the beam Cerenkov counters (2 threshold Cerenkov counters for detection of  $\pi^+$ 's and 2 differential Cerenkov counters CEDAR for detection of K's and  $\bar{p}$ 's). This is performed off-line by requiring the signals from the Cerenkov counters to be in coincidence within a few nanoseconds (4 nsec for the threshold counters and 3 nsec for the CEDAR's) with the T1 counter hodoscope which is used as time reference for each event. There are 12 PM's in T1 and 8 PM's in each CEDAR. All Cerenkov counters and T1 elements have their time information digitized by TDC's. The registered times are readjusted by a suitable time calibration procedure. The time for each detector is then defined in the following way :

a) for the two threshold Cerenkov counters we take the time of the first signal;

b) for each of the two CEDAR's we take the average time of 5-6 photomultipliers after a  $\chi^2$  analysis of the TDC digitization. This results in rejecting those photomultipliers whose time information is too far off from the mean value;

c) for the T1 hodoscope we take the average time of the two elements that have detected the muon pair. This time is used in the subsequent analysis as reference time.

Identification of  $\pi^+$ 's by the threshold Cerenkov counters is illustrated in fig. 7a which shows the time distribution of the signals after subtraction of the reference time. Region II of 4 nsec width shows a clear peak due to all  $\pi^+$ 's (overall detection efficiency of 98%); region III shows pions arriving after the triggering interaction; region I contains events for which a pion, different from the particle responsible for the trigger, has traversed the experiment between 2 and 15 nsec earlier, these events are used to estimate the dead time losses which are typically of 30%. Extrapolation of the region III under the peak of region II allows subtraction of random coincidences.

Identification of  $K$ 's and  $\bar{p}$ 's by the two CEDAR's is illustrated in fig.7b in the case of  $K^-$  at 150 GeV/c. It shows the time distribution of the signals from the CEDAR after subtraction of the reference time. The  $K^-$  events giving the trigger are contained in the peak and represent 3.5% of the overall flux of  $5 \times 10^7$  particles per 800 msec of effective spill time. Random events under the peak produce a contamination of typically 30%.

#### 9.5 Processing time

The complete processing of one event (including filling histograms, tests of the detectors and DST writing) takes about 25 milliseconds on a CDC 7600 computer. This allows a very fast processing of the total data sample.

It should be noticed that about 60% of the triggers are fully reconstructed dimuon events. This proves the cleanliness of the trigger.

#### 9.6 Acceptance

The acceptance of the spectrometer has been determined from Monte-Carlo simulation of dimuons, taking into account the production mechanism of these events, and the complete field map of the magnet.

Fig. 8 shows the acceptance as a function of various kinematical variables, for a 200 GeV/c incoming beam. As can be seen, the acceptance is fairly good for high masses (about 35% for masses above  $7 \text{ GeV}/c^2$ ). The large  $x_F$  acceptance, which is much better than that of previous experiments, allows within the framework of the Drell-Yan mechanism a good determination of the structure functions of beam and target particles(3).

### 10. CONCLUSIONS

The above described spectrometer has proven the following features :

- a high degree of reliability of all detectors and of the data acquisition system

- a powerful, high rejection trigger system which allowed to select good events with a low background contamination; this was mostly due to the  $p_T^V$  cut performed by the matrix logics.

- a fast and efficient off-line processing of the data, allowing the full analysis of several millions of triggers in a few weeks.

Various other configurations of the spectrometer have been tested and prepared for future experiments. They include : a) the use of a new version of the matrix logics performing on-line calculation of the dimuon mass, thus sharpening the mass cut and increasing the rejection power of the trigger; b) operation of large acceptance threshold Cerenkov counters for identification of secondaries in the spectrometer; c) operation of a fine grain 3 stage electron calorimeter for electron-pion separation; d) on line pattern recognition hard processor<sup>(25)</sup>.

#### Acknowledgements

Several teams and people have contributed at the various stages of the experiment. We wish to thank especially :

- all the technical and engineering staff of the collaboration, for the design, construction and operation of all the detectors, components and computer programs of the experiment;

- the staff of the computer centers at CERN, Saclay and IN2P3 (Paris) for the efficient processing of a large amount of data;

- the SPS operation group who has delivered remarkably stable extracted beam over the long period of operation of our spectrometer;

- the Experimental Areas group of CERN, for its constant assistance and especially P.L. Coet and N. Doble who have provided the secondary beam in several different configurations according to the needs of the experiment;

- the Saclay maintenance group directed by G. Bertalmio for their important contribution to the set-up modifications and improvements;

- all the members of the crane crew of the EHN1 experimental hall for their unconditioned and efficient help provided for the several changes of spectrometers and beam configurations;

- our group-secretary for her invaluable assistance in several group activities.

## REFERENCES

- (1) J. Badier et al., Phys. Lett. 86B (1979) 98.  
J. Badier et al., Dimuon resonance production from 200 and 280 GeV/c tagged hadron beams, EPS International Conference on High Energy Physics, Geneva 1979; CERN/EP Preprint 79-61.
- (2) J. Badier et al., Muon-pair production at masses above 5 GeV (Drell-Yan Continuum), EPS International Conference on High Energy Physics, Geneva 1979; CERN/EP Preprint 79-68.
- (3) J. Badier et al., Experimental determination of the pion and nucleon structure functions by measuring high-mass muon pairs, Proceedings of the EPS International Conference on High Energy Physics, Geneva 1979, CERN, Geneva Ed. p 751.  
J. Badier et al., Phys. Lett. 89B (1979) 145.
- (4) C. Bovet et al., IEEE Trans. Nucl. Sci. NS 25 (1978) 572.
- (5) N. Doble, Secondary beams in the north experimental area, in SPS Experimenters handbook 1978 p. 59, CERN SPS Division.
- (6) V. Agoritsas, Proceedings of Symposium on beam intensity measurements Daresbury, 22-26 April 1968, p. 117-151.
- (7) A.L. Grant, Nucl. Instr. and Methods 131 (1975) 167.
- (8) M. Morgurgo, Cryogenics 19 (1979) 411.
- (9) A. Diop, Thèse Université de Paris-7, May 1979.
- (10) R. Hammarström, Multiwire proportional chamber preamplifier for high counting rates, CERN Internal Report NP 75-6.
- (11) Delay, gate and memory monolithic chips, type RBB manufactured by EFCIS, Grenoble.
- (12) R. Hammarström et al., Large multiwire proportional chambers for experiment NA3 at the CERN SPS; Submitted to Nucl. Instr. and Methods 1980. (CERN EP Preprint 80-12)  
R. Hammarström, A large multiwire proportional chamber and associated electronics used in the NA3 experiment at high particle rates; CERN EP Internal Report 79-11.
- (13) G. Burgun et al., Very large multiwire proportional chambers for the NA3 experiment, Saclay DPHPE 79/13.
- (14) LRS PC-800, developed and fabricated by LeCroy Research System Corporation, Spring Valley, NY, USA.
- (15) JCF20 read-out module, Schlumberger SA, Paris, France.

- (16) J. Boucrot et al., A trigger system using cathode readout chamber and a coincidence matrix; LAL Orsay 79/33; submitted to Nucl. Instr. and Methods.  
R. Dubé, Thèse Université d'Orsay, LAL-79/6, March 1979.
- (17) PDP 11/45 with 48 K of 16 bit words memory running a modified RT11 operating system. This operating system occupies 4K words memory, (A. Katz, Private communication, Saclay-DPhPE).  
A. Compant Lafontain, Thèse Université de Paris VII, May 1979.
- (18) B. Ollivier, Systeme d'acquisition des données en spectrometrie généralisée. Journées d'information electronique (15-17 avril 1975) CEN-Saclay.
- (19) R. Marbot, A. Simon and C. Violet, Ensemble de compactage lecture d'ADC, LPNHE-Ecole Polytechnique, Paris 1977.
- (20) J.C. Brisson et al., An efficient data acquisition system for the NA3 experiment, (to be published).
- (21) M. Handroul, Physics algorithms and programs; CERN Program Library X999, entry S3101 (1978).
- (22) R. Brun, R. Hagelberg and J.C. Lassalle; GEANT : CERN/DD/78/2 (1978).
- (23) R. Brun, M. Hansroul, J. Kubler and H. Wind; MUDIFI, Multi-dimensional fit program, CERN/DD/US/69 (1980).
- (24) J.G. Branson et al., Phys. Rev. Lett. 38 (1977) 1334 and reference therein.
- (25) M. Mur; Morpion : a hard processor for straight track finding; Paper presented at the Wire Chamber Conference, Vienna 1980.

TABLE 1

Beam characteristics for the NA3 experiment. The beam spot size at the experiment is smaller than 12 mm diameter at all energies. The intensities indicated in the second column were used with an effective spill time of 0.8 sec average.

Energy (GeV)	Total beam intensity per $3 \times 10^{12}$ protons of 400 GeV on T4 beryllium target.	Beam production angle (mrads)	T4 target length (cm)	Beam composition (%)	Signature of beam particles	Remarks
-280	$1 \times 10^7$	0	50	$> 99. \pi^-$	none	-
-200	$3 \times 10^7$	0	50	$96.3 \pi^-$ $3.1 K^-$ $0.6 \bar{p}$	one CEDAR on $K^-$ one CEDAR on $\bar{p}$	-
+200	$5.5 \times 10^7$	0	50	$36. \pi^+$ $60. p$ $4. K^+$	2 CEDAR's on $K^+$ 2 threshold Cerenkov on $\pi^+ + K^+$	2m CH <sub>2</sub> filter
-150	$5 \times 10^7$	2-4	30	$93. \pi^-$ $5. K^-$ $2. \bar{p}$	one Cedar on $K^-$ one CEDAR on $\bar{p}$	-
+400	$10^9$ (with 3,4 m beam dump)	-	-	100. p	-	extracted proton beam attenuated by a 3.8m Be absorber.

TABLE 2

Geometrical characteristics of the NA3  
proportional chambers.

Proportional chamber units	Sensitive area (m <sup>2</sup> )	Angle $\theta$ of sense wires with respect to vertical direction (degrees)	Number of planes	Number of wires per plane	Wire spacing (mm)
PC1	0.64x0.64	0	2	320	2
		90	2	320	2
		45	1	320	2.83
		135	1	320	2.83
PC2	circular $\phi$ 1.344 m	0	2	448	3
		90	2	448	3
		45	1	448	3
		135	1	448	3
PC3 + PC4	3.1x2.6	0	4	1024	3
		90	4	864	3
		15	2	1024	3
		165	2	1024	3
PC5 + PC6	4.25x4.05	0	5	1408	3
		90	2	1344	3

TABLE 3

Trigger rates at 200 GeV

	positive beam	negative beam
Total beam flux per burst	$2 \times 10^7$	$3 \cdot 10^7$
Pretrigger	$3 \times 10^4$	$8 \times 10^4$
Trigger (1+2)	~20	~50

## FIGURE CAPTIONS

- Fig. 1 General layout of the NA3 experiment,  
T1, T2, T3 : Trigger hodoscopes  
M1, M2 : Trigger chambers  
PC1,.....,PC6 : Proportional chambers.
- Fig. 2 Elements of the trigger system.
- Fig. 3 The hadron absorber with its central heavy plug.
- Fig. 4 Electronics of the trigger system.
- Fig. 5 Principle of the data acquisition system.
- Fig. 6 Off-line reconstruction of events : vertex of dimuons with  $M_{\mu\mu} > 5 \text{ GeV}/c^2$ .
- Fig. 7 a) Time spectrum of threshold Cerenkov counters for  $\pi^+$  identification; Region I, II and III are defined in § 9.4c);  
b) Time spectrum of CEDAR counters for  $K^-$  identification : plotted in the time mean value of the 5 photomultipliers (the structure of 200 MHz visible in the histogram is due to imperfect debunching of the SPS at ejection). More than 95% of the kaons are in a 3 nsec interval.
- Fig. 8 Acceptance of the spectrometer for 200 GeV/c incoming particles,  
a) as a function of  $x_F$ , for different dimuon masses;  
b) as a function of the transverse momentum  $p_T$  of the dimuon;  
c) as a function of  $M_{\mu\mu}$ ;  
In fig.8c the mass resolution  $\sigma_m$  is also given, as a function of  $M_{\mu\mu}$ . The measured value of the mass resolution for the  $J/\psi$  is also given.
- Fig. 9 Dimuon mass spectrum produced by incident  $\pi^+$  of 200 GeV/c. The  $\psi$  and  $\gamma$  signals are seen at 3.1 and 9.5 GeV respectively. The  $\frac{\mu^+\mu^+ + \mu^-\mu^-}{2}$  points show the level of background.

CERN NA 3 SPECTROMETER

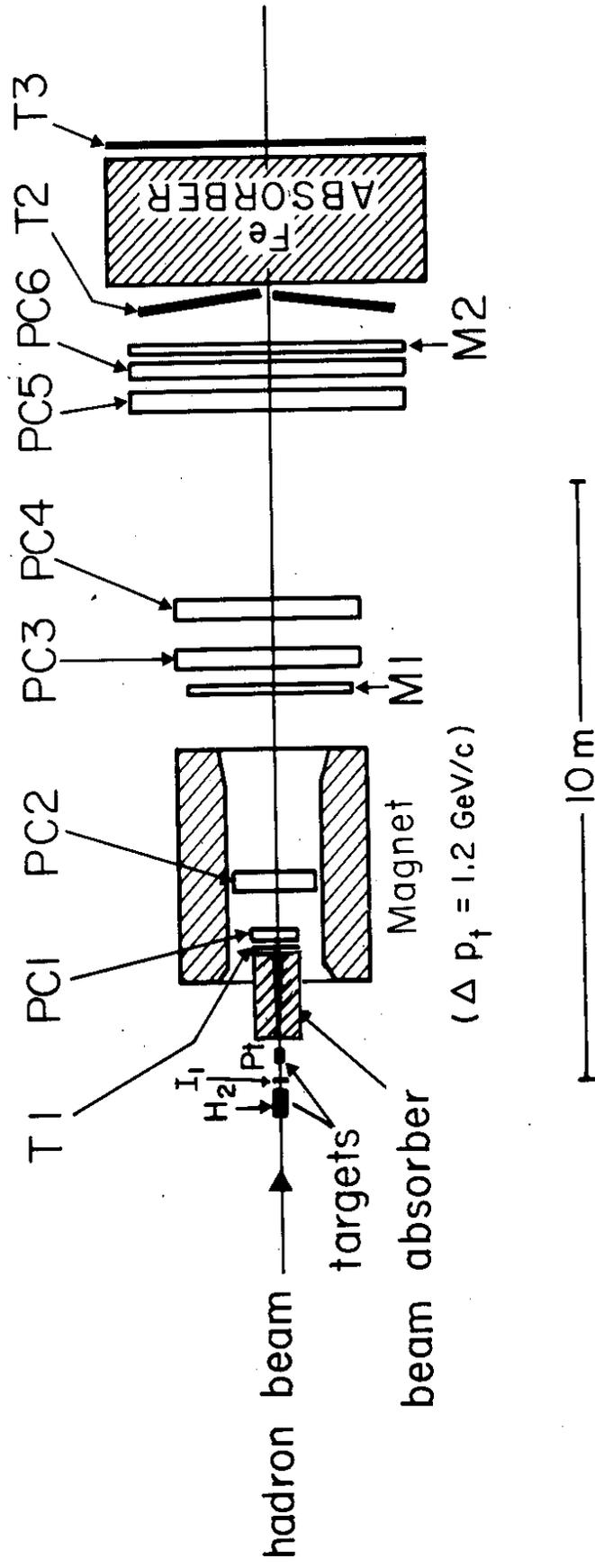


FIG. 1

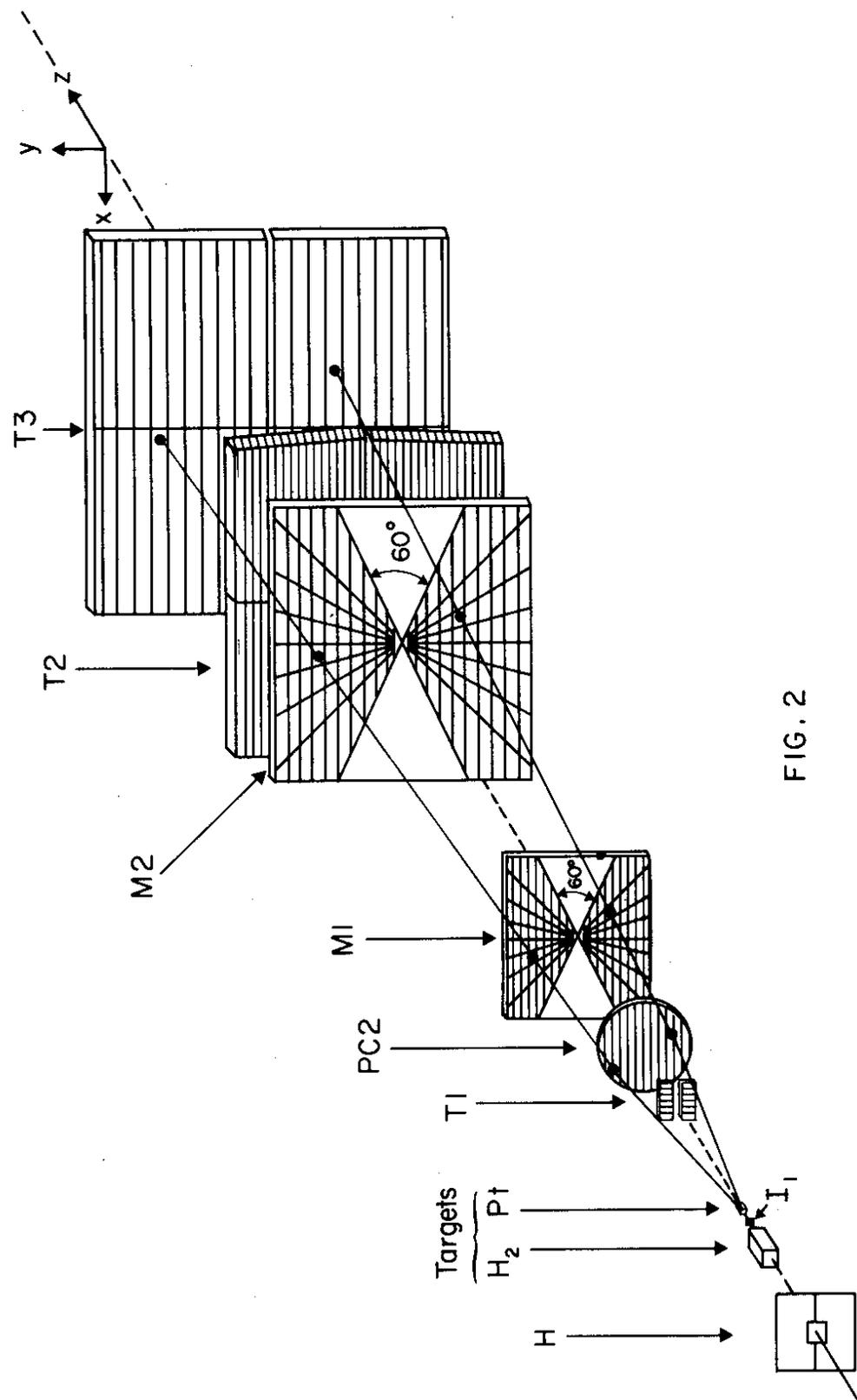


FIG. 2

HADRON ABSORBER

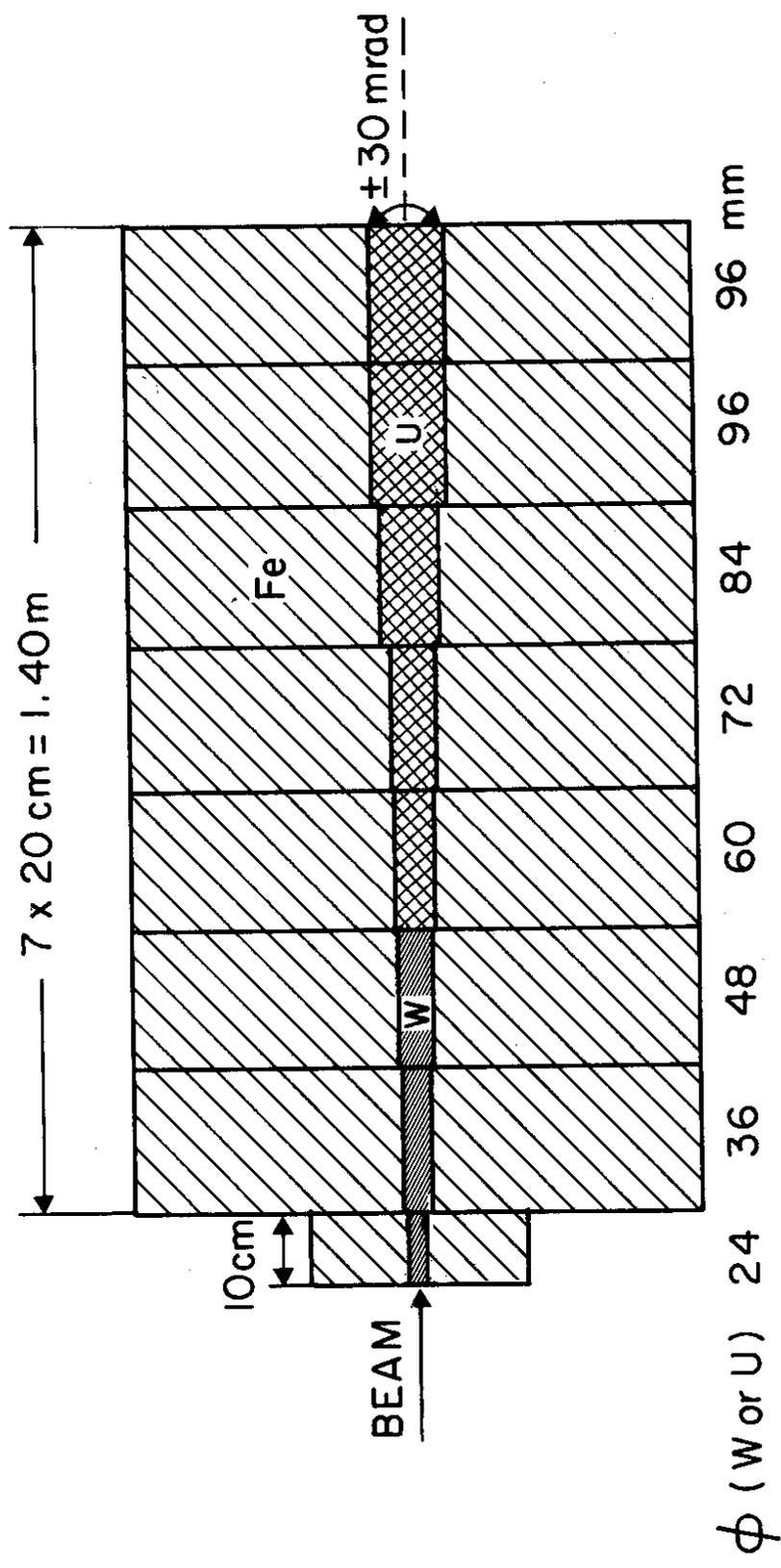


FIG. 3

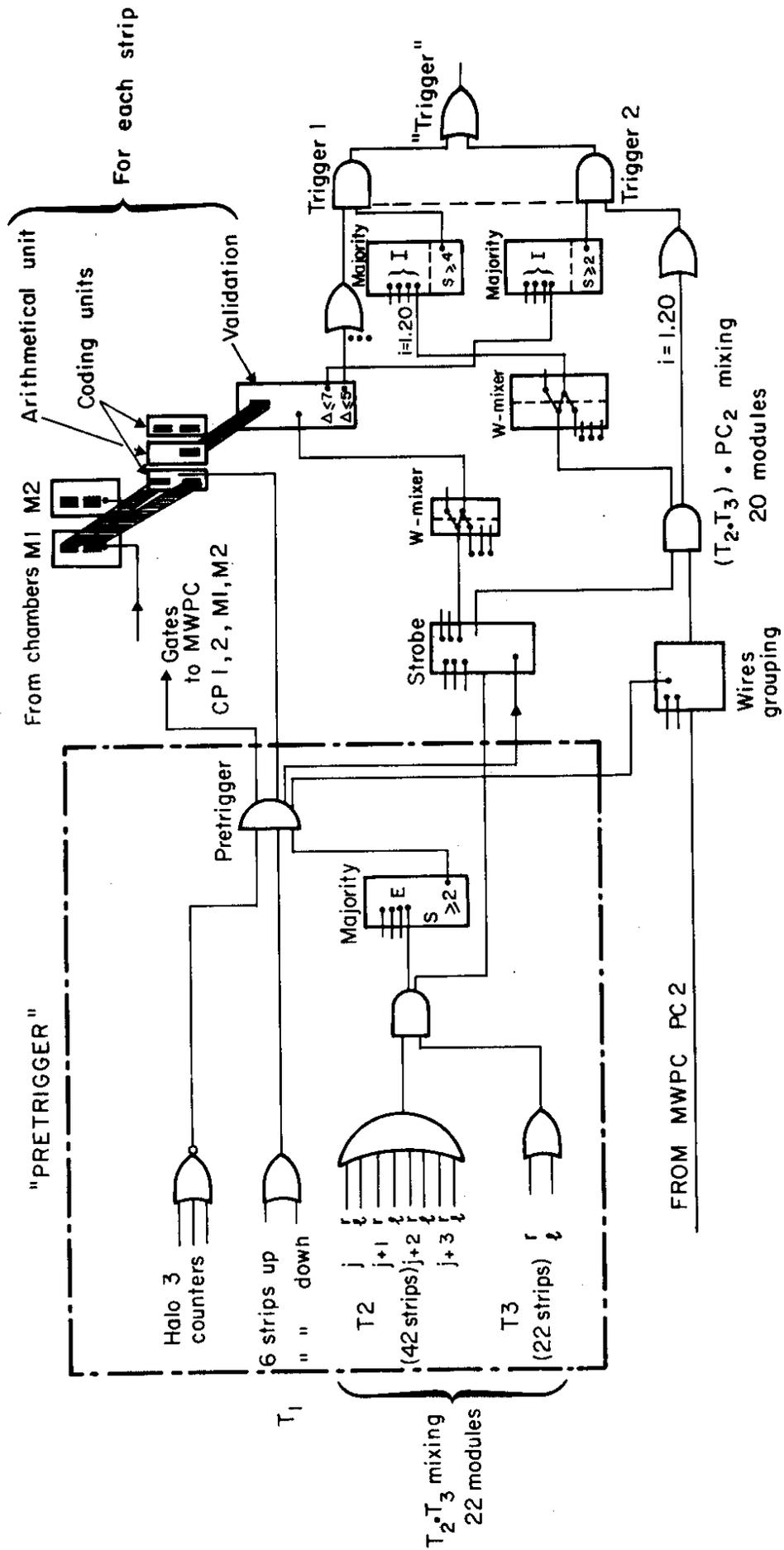


FIG. 4

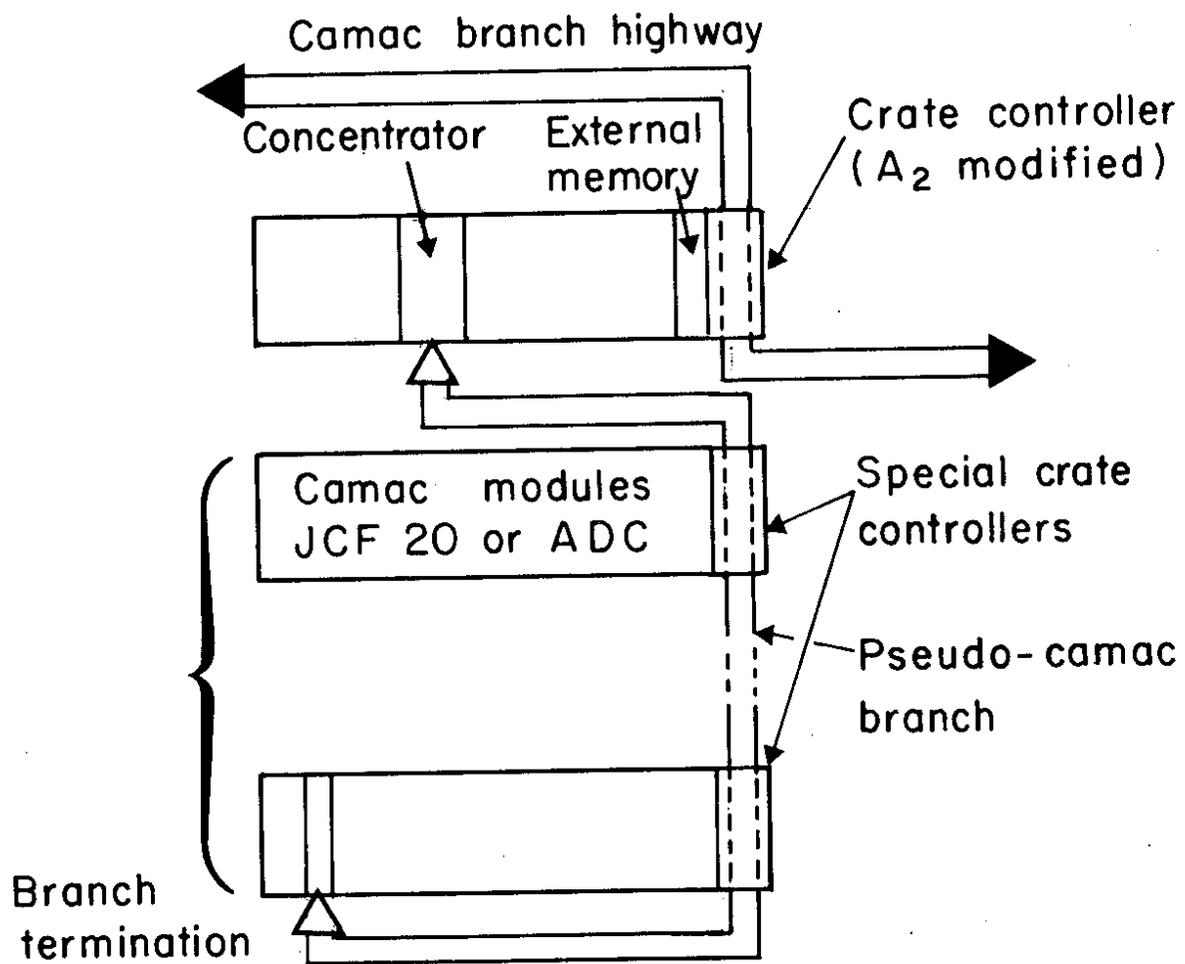


FIG. 5

# Vertex Reconstruction

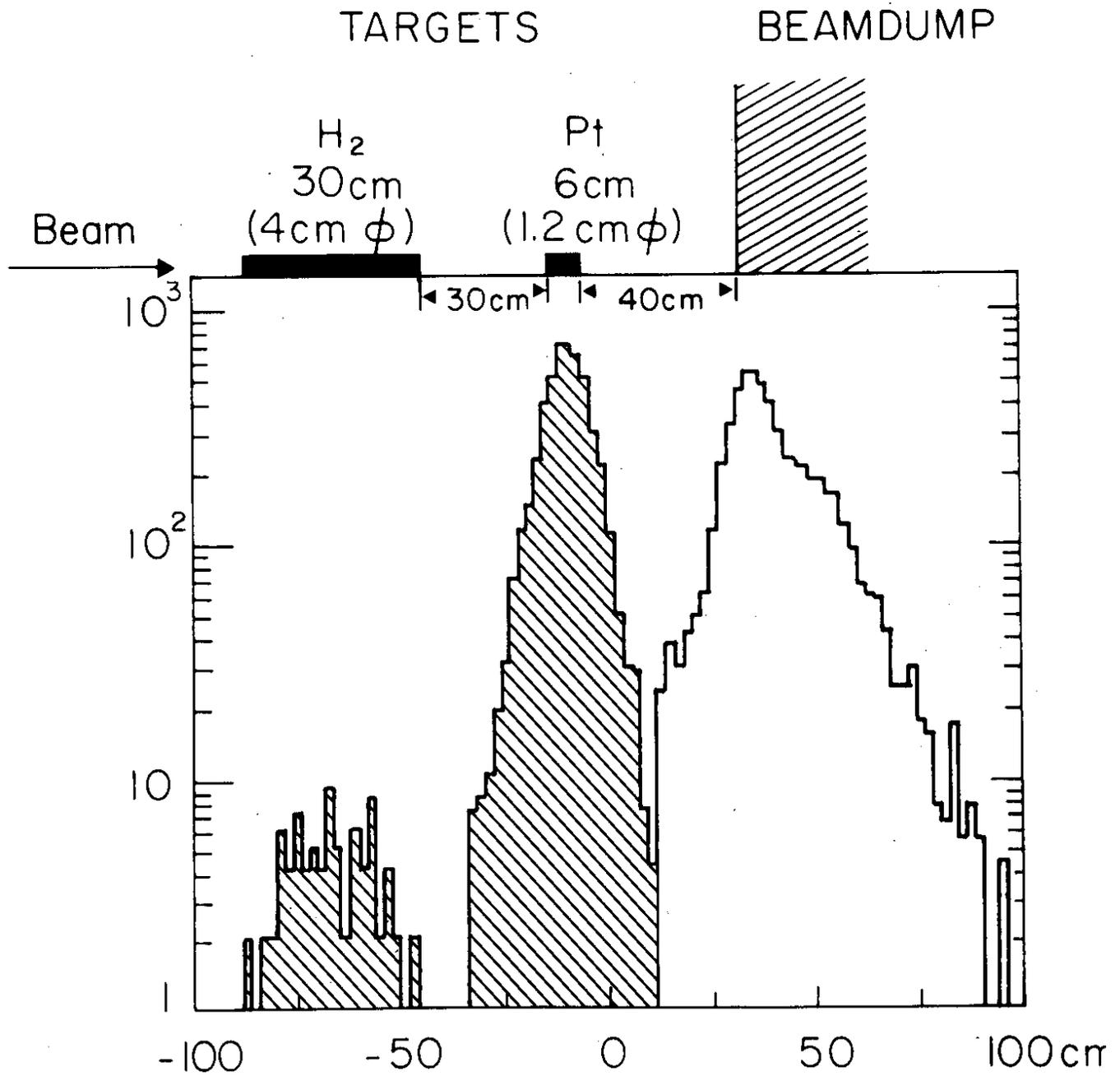


FIG. 6

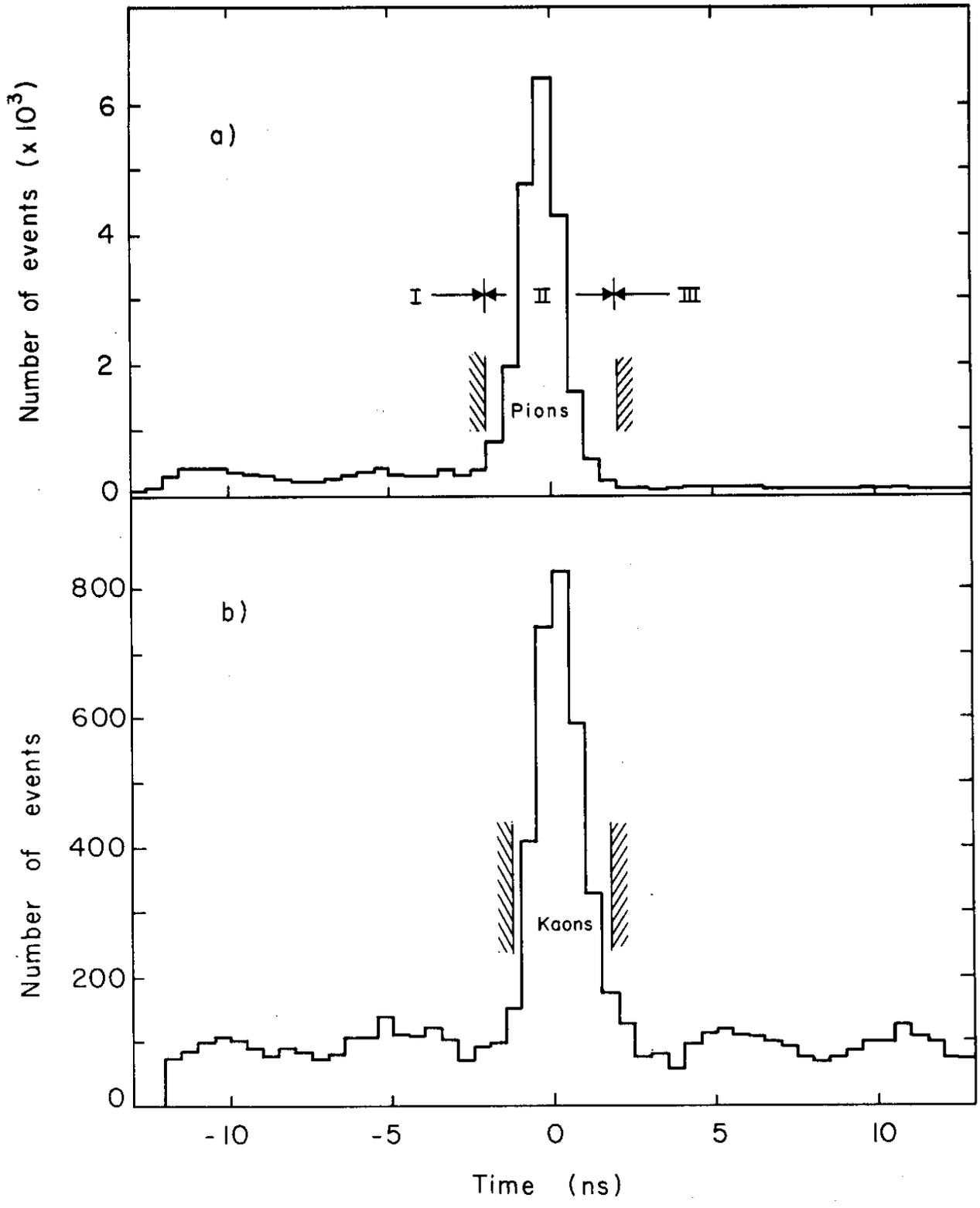


FIG. 7

# ACCEPTANCE

IN  $X$ ,  $P_T$ ,  $M_{\mu\mu}$  at 200 GeV/c

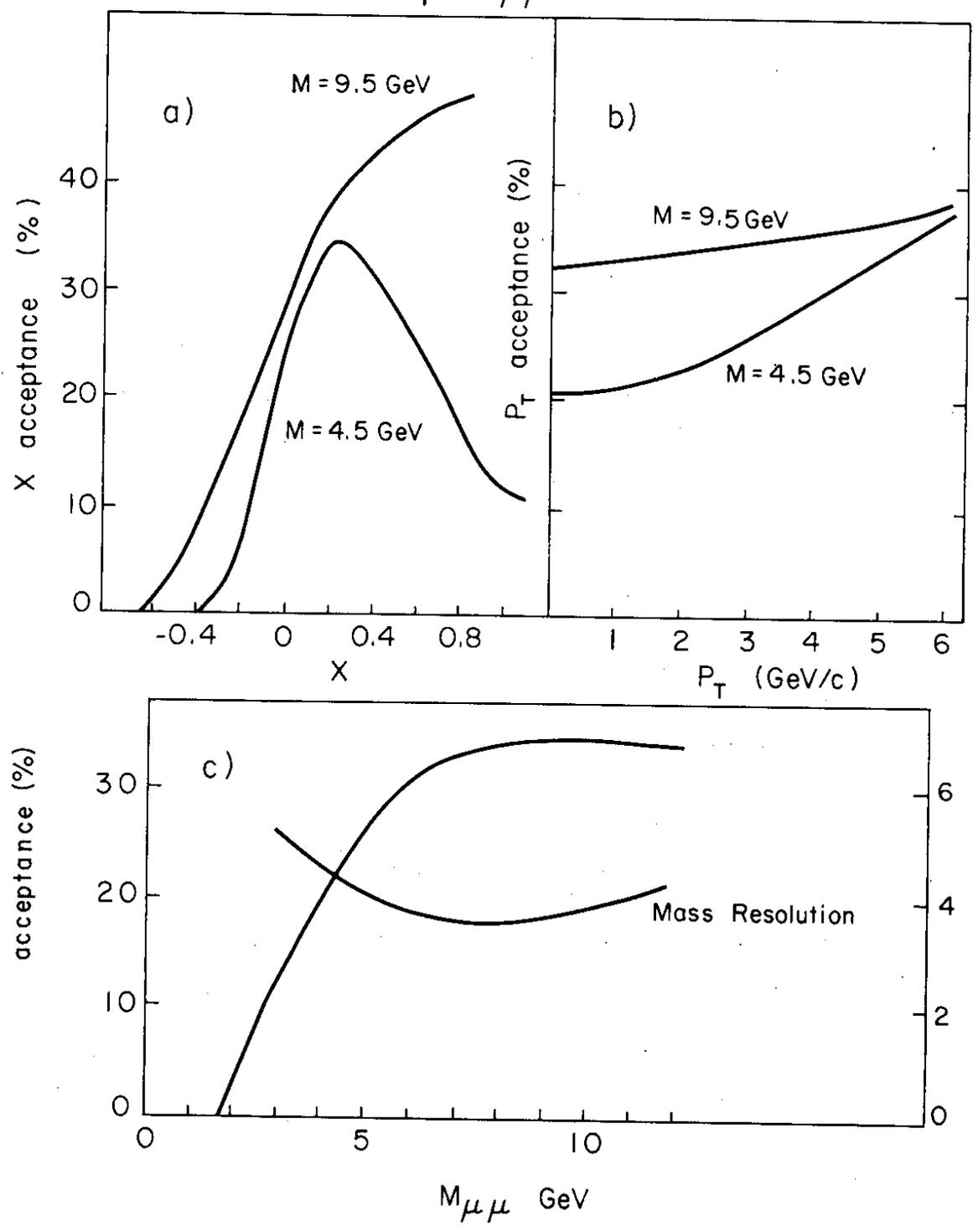


FIG. 8

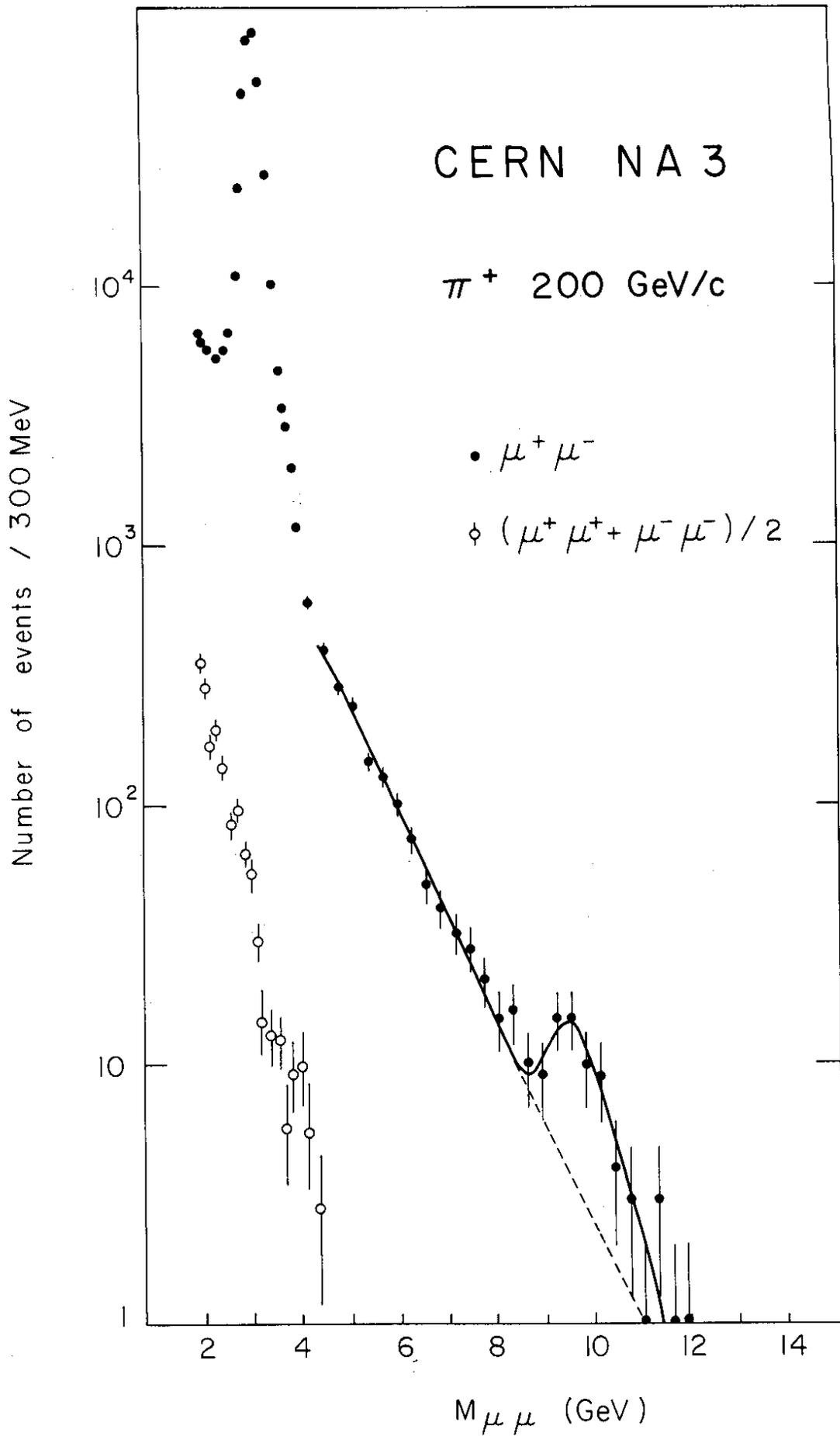


FIG. 9

